SISSA

TECHNICAL REPORT • OPEN ACCESS

Performance comparison of water Cherenkov detectors with different geometries

To cite this article: F. Bisconti and A. Chiavassa 2023 *JINST* **18** T07003

View the article online for updates and enhancements.

TECHNICAL REPORT

Performance comparison of water Cherenkov detectors with different geometries

F. Bisconti[1,*] **and A. Chiavassa**

University of Turin and INFN Section of Turin,
Via Pietro Giuria 1, Turin, Italy

E-mail: francesca.bisconti@to.infn.it

ABSTRACT: In the framework of the development of the SWGO experiment, we have performed a detailed study of the single unit of an extensive air shower observatory based on an array of water Cherenkov detectors. Indeed, one of the possible water Cherenkov detector unit configurations for SWGO consists of tanks, and to reach a high detection efficiency and discrimination capability between gamma-ray and hadronic air showers, different tank designs are under investigation. In this study, we consider and compare double-layer tanks with several sizes, shapes and number of photo-multiplier tubes (PMTs). Muons, electrons, and gamma-rays with energies typical of secondary particles in extensive air showers have been simulated entering the tanks with zenith angles from 0 to 60 deg. The comparison between different tank geometries was evaluated considering the number of photoelectrons produced by the PMTs, the detection efficiency, and the time resolution of the measurement of the first photon. We will show that with circular and hexagonal tanks better performance can be obtained than with the square ones, and that it improves for smaller tanks as expected.

---

[1]Now at INFN Section of Roma Tor Vergata.
[*]Corresponding author.

Contents

1 Introduction

Wide field of view gamma-ray observatories can be realized by an array of water Cherenkov detectors, covering areas ranging from 10^4 to 10^6 square meter, usually located in desertic areas. Secondary particles produced in extensive air showers induced by astrophysical gamma-rays or hadrons (that in this case represent a background source), can be detected measuring the Cherenkov light produced when they cross the detectors filled with clean water. A next-generation gamma-ray experiment is the Southern Wide-field Gamma-ray Observatory (SWGO) [1, 2], which will be realized at high altitude in the Southern Hemisphere, to be complementary to other gamma-ray experiments in the Northern Hemisphere, like HAWC [3] and LHAASO [4], for the observation of the entire sky. It will operate with close to 100% duty cycle and on order a steradian field of view. The site has to be at high altitude (above 4 400 m a.s.l.), in order to be closer to the maximum of the extensive air showers induced by astrophysical gamma-rays with primary energy in the range of interest (between 100 GeV and a few PeV). The SWGO design will be primarily based on water Cherenkov detectors, and the final array and detector unit configurations are still to be defined [1]. One configuration under study consists of and array of (surface) water Cherenkov tanks arranged in a high fill-factor core (with an area considerably larger than that of the HAWC experiment) and a low density outer array.

To study the single tank behaviour, we performed simulations of particles crossing tanks with different size and configuration of PMTs. We simulated double-layer tanks (DLT) [5], in which the lower layer helps in the gamma/hadron discrimination, as muons are more abundant in hadronic

showers and they can cross the upper layer reaching the lower layer where they can be measured. We considered tanks of different shape, with circular (Circular-DLT), hexagonal (Hexagonal-DLT) and square (Square-DLT) base.

To simulate the particles crossing the tanks and their response, we used the HAWCSim framework[1] [6], which makes use of GEANT4 [7] to simulate the interaction of the particle with the tank itself and the water volume, including the production of the Cherenkov photons that can be detected by the PMTs inside the tank.

2 Simulations

2.1 Particles

In this analysis, we considered the most abundant particles contained in an extensive air shower generated by 400 GeV protons and 200 GeV photons at an observation level of 4 500–5 000 m a.s.l. Therefore, we performed simulations of electrons, gamma-rays and muons with fixed energies: 10 MeV, 100 MeV and 1 GeV electrons and photons, and 1 GeV and 10 GeV muons. To define the directions, we used azimuth angles ϕ uniformly distributed in the range 0–360 deg and zenith angles θ in the range 0–60 deg sampled on a $\cos^2 \theta$ distribution.

The particles were generated on a large circular surface 10 cm above the tank and centered with it. The size of the generation area is such that even the most inclined particles could enter the tank from the lateral walls of the upper layer, to avoid the detection of particles entering in the tank directly from the lower layer that would affect the overall performance of a single tank study. This has to be considered in the context of a sparse array of tanks, while in a dense array the nearby tanks contribute to the detection capability of the large-scale experiment. Therefore, for each tank design, particle type and energy, 10000 particles entering the upper layer of the tanks have been analyzed.

2.2 Specifications of the tanks

2.2.1 Shapes and dimensions of the tanks

In this analysis, Circular-DLTs, Hexagonal-DLTs and Square-DLTs were considered. In figure 1 examples of the Geant4 visualization of the three tank designs crossed by a muon are shown.

The height of the upper layer was chosen allowing the Cherenkov photons to reach any PMT at the base of the upper layer. Assuming a vertical particle entering the tank from the center of the roof, the Cherenkov photons should be able to reach the lateral walls of a Circular-DLT or the corners of an Hexagonal-DLT and a Square-DLT at the base of the upper layer. For Circular-DLTs the height h and radius r follow the relation $h = r/\tan\theta_C$, where $\theta_C = 41.2$ deg is the emission angle of the Cherenkov photons with respect to the trajectory of the particle crossing the water. Similarly, for Hexagonal-DLTs with side L, the height is $h = L/\tan\theta_C$, and for Square-DLTs with half side l, $h = \sqrt{2}l/\tan\theta_C$. To the height calculated with previous formulas, 1 m of water is added to have 90% probability that gamma-rays interact by pair production. The lower layer, with height independent of the radius, is dedicated to muon measurements, allowing for the gamma/hadron discrimination and the separation of mass groups of charged primaries (from 2 to 4). For the lower layer, we chose heights of 0.5 m, 0.75 m and 1 m. The dimensions of the tanks are collected in table 1.

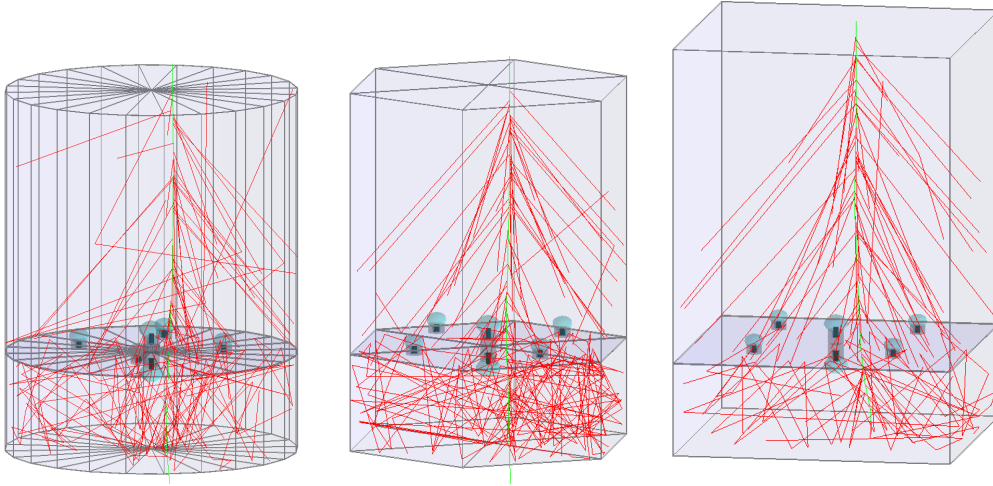[1]HAWCSim was developed for HAWC and then adapted to SWGO.

Figure 1. Geant4 visualization of a Circular-DLT, an Hexagonal-DLT and a Square-DLT, crossed by a 1 GeV vertical muon. All tanks have widths of 3 m (diameter for Circular-DLT, two times the side for Hexagonal-DLT, and side for Square-DLT) and lower layers 1 m high. The upper layers were simulated with non-reflective walls, while the lower layer with reflective walls. The green line represents the simulated muon and the red lines a sample of Cherenkov photons.

Table 1. Size of the simulated tanks. "Width" is the diameter of Circular-DLTs, the side of Square-DLTs and two times the side of Hexagonal-DLTs; "Cyl.&Hex. Height u.l." is the height of the upper layer of Circular-DLTs and Hexagonal-DLTs; "Sqr. Height u.l." is the height of the upper layer of Square-DLTs; "Height l.l." is the height of the lower layer.

Tank	Width (m)	Cir.&Hex. Height u.l. (m)	Sqr. Height u.l. (m)	Height l.l. (m)
T1	3	2.7	3.4	0.5, 0.75, 1
T2	3.5	3.0	3.8	0.5, 0.75, 1
T3	4	3.3	4.2	0.5, 0.75, 1
T4	4.5	3.6	4.6	0.5, 0.75, 1
T5	5	3.9	5.0	0.5, 0.75, 1
T6	5.5	4.2	5.4	0.5, 0.75, 1

The tanks are made of steel, 6 mm thick. As the DLTs are simulated as two overlapped compartments, the divider between the upper and lower layers results to be 1.2 cm thick. The inner surface of the tanks have covers with different optical properties, depending on the wanted reflective capabilities (see section 2.2.2).

2.2.2 Properties of the inner walls

For the inner walls of the upper layers, we used both reflective (Tyvek) and non-reflective (Polypropylene) materials. The reflectivity of the materials depends on the wavelength of the incident photons. Tyvek has a reflectivity of 0.63–0.92 in the wavelength range 250–650 nm; polypropylene has a reflectivity of 0.10 over the same wavelength range. Reflections occurring on both the materials are diffuse reflections. Reflective walls allow for a better detection capability, but might extend the detection time, due to possible consecutive reflections of photons on the walls before they reach

the PMTs. This results in a higher detection efficiency as photons that would not be detected with non-reflective walls are instead detected with reflective walls, but also widens the time resolution for the detection of the first photon. For the lower layer we used reflective walls, as the priority was given to the detection efficiency of particles entering the lower layer rather than the timing.

2.2.3 PMTs

In the upper layer, we used two configurations of PMTs looking upwards: one central 10″ PMT or four peripheral 5″ PMTs placed at half radius in Circular-DLTs, half the apothem in Hexagonal-DLTs, and half diagonal in Square-DLTs. Signals of the peripheral PMTs are summed in one unique output. In the lower layer we used one central 10″ PMT or 5″ PMT looking downwards. In each layer, the two PMT configurations have to be considered independently. In the simulations, we used two models of PMTs from Hamamatsu: the 10″ R7081HQE PMT, and the 8″ R5912 PMT, then re-scaled to a 5″ PMT during the analysis phase. The quantum efficiency of the PMTs has been taken from the datasheet [8], while the transit time spread is simulated with a simple smearing of 1 ns. The dark noise of the PMTs was not considered in this study, we just applied a conservative trigger threshold in the absence of simulated noise.

3 Analysis

For the evaluation of the tank response, the parameters taken into account are:

- The number of photoelectrons (PEs) produced in both layers. In the upper layer we considered separately the configuration with one central 10″ PMT or four peripheral 5″ PMTs. For the lower layer we considered individually a central 10″ PMT or 5″ PMT. This allowed to understand which of the two configurations in the upper layer gives the higher detection efficiency and the better time resolution of the first detected photon and, for the lower layer, how the size of the PMT influences the detection efficiency, which is expected to be higher for muons that reach more easily the lower layer.

- The time resolution of the measurement of the first photon in the upper layer, evaluated as the standard deviation of the distribution of the first photon arrival time. In real experiments the particle arrival time in each tank is usually measured fitting the shape of the PMT signal. In the HAWCSim framework used for the simulations this was not implemented. Therefore, we considered the arrival time of the first PE (although in real experiments it can be influenced by various noise sources) that is a clearly defined parameter in the simulation outputs and that can be used to compare the different tank geometries.

- The detection efficiency of both layers. The efficiency is calculated as the number of detected particles (events) divided by the number of particles entering the upper layer of the tank (10000). The latter is based on simple geometrical considerations, based on the height of the entrance point of the particles. Due to the random direction of the particles, a fraction of those entering the upper layer does not enter the lower one. We tried to evaluate the number of particles actually entering the lower layer based on the initial direction of the particles, but this was not possible due to non-tracked deflections of the particle trajectories occurring while

they cross the tank. To verify this, we performed a set of simulations where only 10 GeV vertical muons were thrown through a Circular-DLT, and in this case the detection efficiency was ∼ 1 for both the upper and lower layer. This demonstrated that the inefficiency of the lower layer is only due to geometrical constraints, and would be effectively reduced considering a joint detection of inclined particles by neighbouring tanks in a dense array. Therefore, also in the calculation of the detection efficiency of the lower level we used as reference the number of particles entering the upper layer of the tank. This underestimates the detection efficiency of the lower layer for any type of tank and particle, but the comparison between the different configurations remains valid. For the upper layer, we considered as threshold both 1 PE and the coincidence of 2 PEs produced within 30 ns by the central 10″ PMT or by the four peripheral 5″ PMTs, while for the lower layer the threshold was only of 1 PE. We chose such low thresholds in order to increase the detection efficiency at the low energies and referring to the experience of the HAWC experiment [9].

In figure 2 sample distributions of the number of PEs (a–c), the arrival time of the first photon (d–f), and the arrival time of all photons (g–i) of are shown. They refer to simulations of 1 GeV electrons, gamma-rays and muons crossing a Circular-DLT with size corresponding to "T1" in table 1, non-reflective walls in the upper layer and reflective walls in the lower layer.

The information that can be extracted from these plots are listed below, based on the parameter they are referred to.

Number of PEs.

- The distributions for the lower layer has a higher average for muons than for electrons and gamma-rays, as the latter are absorbed by the water of the upper layer.

- The PE distributions also show that particles generate on average more PEs on the central 10″ PMT than on the four peripheral 5″ PMTs.

Arrival time of the first photon.

- The distributions are in general similar. In the sample of distributions reported, the timing resolution for the four peripheral PMTs is slightly narrower than for the central PMT.

- The width of the first photon arrival time distribution is influenced by the path the particles, which are generated with random direction over the tank, travel in water before the Cherenkov emission.

Arrival time of all photons.

- These distributions are also presented to show the effect of the reflective walls in the lower layer (green lines). Especially for muons that reach easily the lower layer, a long tail and a bump (at ∼ 44 ns) after the main peak (at ∼ 33 ns) are due to the consecutive reflections on the walls before photons reach the PMT. This effect is more visible when reflective covers are used also for the upper layer, due to the higher statistics of PEs generated in the upper layer. Depending on the distributions of the impact point on the tank and the direction of the particles, a sequence of bumps might appear instead of the tail.
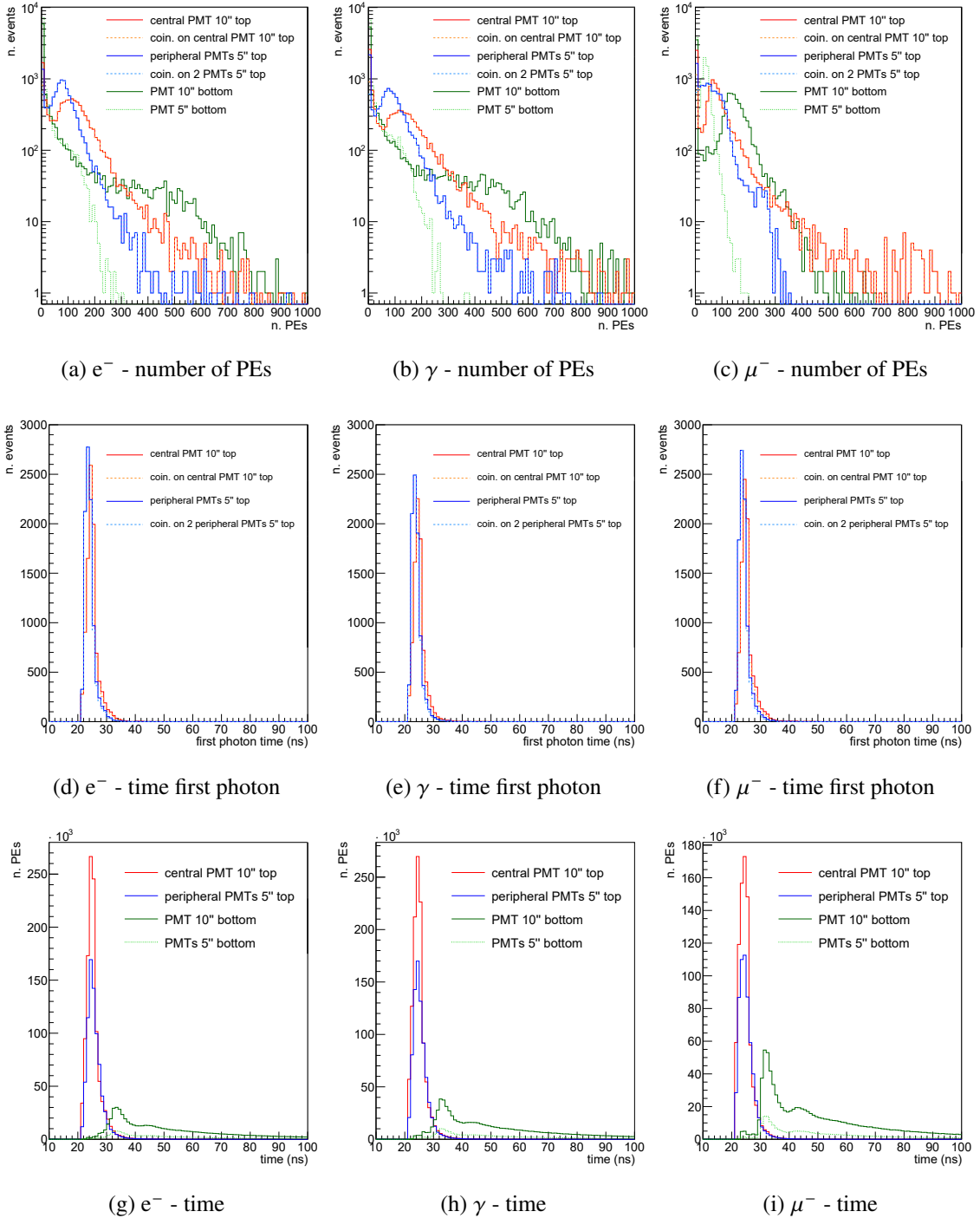
Figure 2. Distributions used in the analysis of the tank performance: number of PEs (a-c), arrival time of the first photon (d-f), and arrival time of all photons (g-i). These plots refer to simulations of 1 GeV electrons, gamma-rays and muons crossing a Circular-DLT with size corresponding to "T1" in table 1, non-reflective walls in the upper layer and reflective walls in the lower layer.

- Effects that influence the time distributions like late-pulsing and after-pulsing are not simulated, therefore plots are not affected by them. The first is a rare phenomenon that occurs with a probability of a few percent [10]; the latter produces PEs many microseconds later and is not considered in the single tank study, although it plays a role in the noise modeling in case of extensive air showers over the entire SWGO array.

4 Results

4.1 Comparison of tanks with different size, reflective properties of the inner walls and PMT configuration

In this section, plots are referred to Circular-DLTs, but the results are similar for all tank geometries. In figure 3–5 the performance of the upper layer is shown, considering a central 10″ PMT or four peripheral 5″ PMTs. Panels (a) are relative to non-reflecting walls, while panels (b) are for reflecting walls. Similarly, in figure 6–7 the performance of the lower layer, which has always reflective walls, is shown considering a 10″ PMT or a 5″ PMT. In the following, the analysis of the performance of the upper and lower layers are listed.

Performance of the upper layers.

- The number of detected PEs (see figure 3) and consequently the detection efficiency (see figure 4) decrease while increasing the size of the tank. This is due to the decrease of the ratio between the area of the PMT and that of the base of the tank. To verify this, we made some test simulations using different tank widths and rescaling the PMT size in order to have a constant ratio between the area of the PMT and the base of the tank, and the detection efficiency remained almost constant.

- With 1 PE threshold, the detection efficiency of the upper layers considering one central 10″ PMT or four peripheral 5″ PMTs are comparable, although more PEs are produced in the central PMT. The sensitive area based on the size of the PMTs is similar for the two configurations. Therefore, the difference is related to the position of the PMTs.

- The efficiency for 10 MeV particles is between 30% and 15% depending on the tank width, while it is above 70% for higher energies and for all tank sizes, reaching values higher than 90% for 1 GeV and 10 GeV particles. With 2 PEs threshold (plots not shown in this work), the efficiency is reduced by a few ten percent for 10 MeV and 100 MeV particles, while it is similar for particles with higher energy.

- With reflective walls in the upper layers, the number of PEs increases by a factor ∼ 3 with respect to the case with non-reflective walls. The detection efficiency for 10 MeV particles reaches values between ∼ 80% and ∼ 50% increasing the tank width, while it is above ∼ 90% for all the higher energy particles (compare figure 3(a) with (b) and figure 4(a) with (b)). Using 2 PEs threshold, the effect is the same as that described for non-reflecting walls.
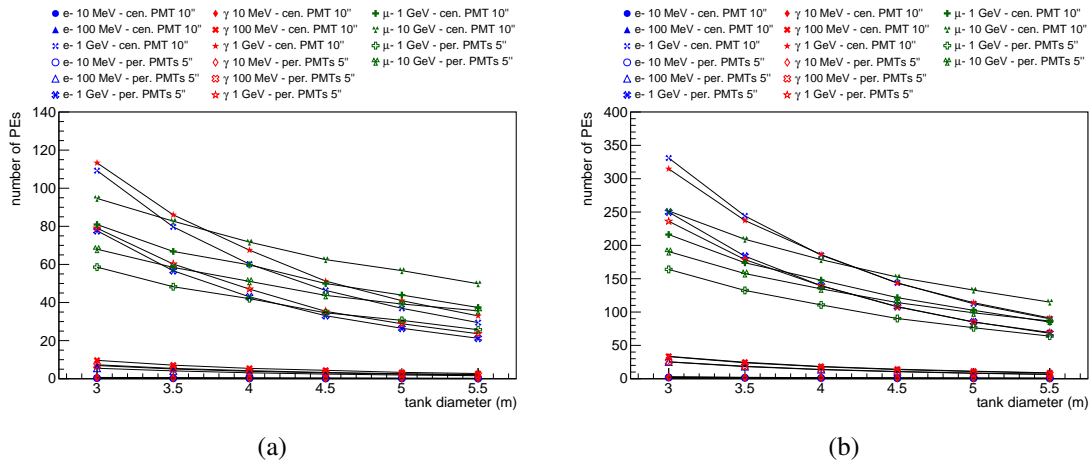
Figure 3. Number of PEs detected in the upper layer of Circular-DLTs with non-reflecting walls (a) and reflective walls (b). Note the different scales on the y-axis.
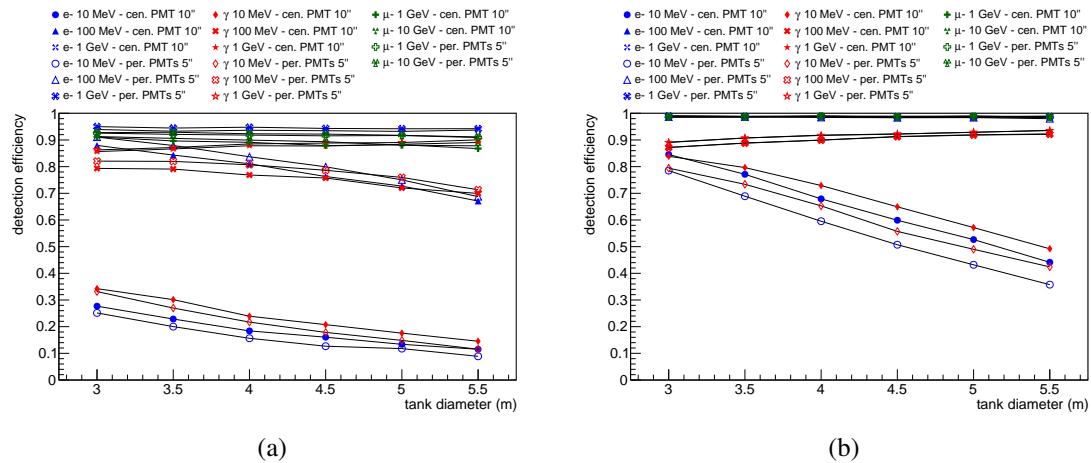

Figure 4. Detection efficiency of the upper layer of Circular-DLTs with non-reflecting walls (a) and reflective walls (b).

- The time resolution of the measurement of the first photon worsen, i.e. the standard deviation of the distribution gets larger, with the increase of the size of the tank (see figure 5). In average, using non-reflecting walls it ranges from ~ 2.5 ns in small tanks to ~ 3.5 ns in large tanks. Considering 2 PEs threshold, it has smaller values, between ~ 1 ns and ~ 2 ns.

- Using reflective walls, the time resolution of the measurement of the first photon slightly increases for 100 MeV and 1 GeV particles, and rises up to ~ 18 ns for 10 MeV particles, because the time distribution of the first photon shows a long tail for these particles. It has similar values for the central 10″ PMT and the four peripheral 5″ PMTs. Considering 2 PEs threshold, it has slightly lower values.
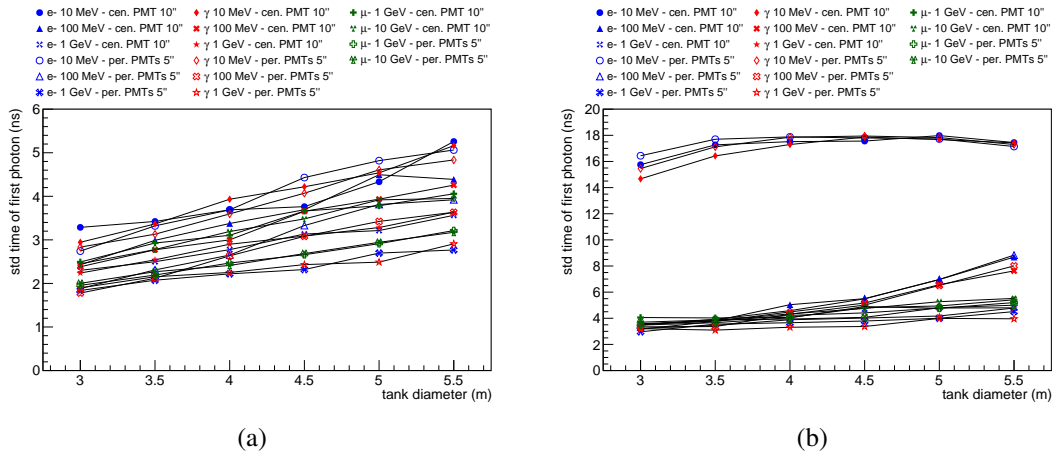
Figure 5. Time resolution of the measurement of the first photon in the upper layer of Circular-DLTs with non-reflective walls (a) and reflecting walls (b).

Performance of the lower layers.

- Like in the upper layer, the number of detected PEs (see figure 6) and the detection efficiency (see figure 7) in the lower layers decrease with the size of the tank.

- Electrons and gamma-rays of 10 MeV and 100 MeV are rarely detected in lower layers, with an efficiency lower than 15%. The detection efficiency for the same particles and with energy 1 GeV varies between ∼ 50% and ∼ 30% increasing the tank width. It is higher for muons: it is ∼ 65% for both 1 GeV and 10 GeV up to tanks with 4 m width, then it decreases for the 1 GeV muons while remains constant for the 10 GeV ones.

- The detection efficiency considering the 5″ PMT is only a few percent lower than that considering the 10″ PMT, although the number of produced PEs in the 5″ PMT is the 25% of that produced in the 10″ PMT, being proportional to the area of the photocathode. Both kinds of PMTs are placed at the center of the ceiling of the lower layer, so there is no effect due to different positioning like it happens in the upper layer.

- The height of the lower layer influences the number of PEs, which is lower for 0.5 m and comparable for 0.75 m and 1 m, but does not affect the detection efficiency (plots not shown in this work).

- In all the configurations, the detection efficiency of the lower layer is underestimated in the same way due to geometrical constraints (see details about the calculation of the detection efficiency in section 3).

4.2 Comparison of tank shapes

The analysis described in the previous section was performed for the three tank shapes of interest: Circular-DLTs, Square-DLTs and Hexagonal-DLTs. In addition to tanks with circular base, which is
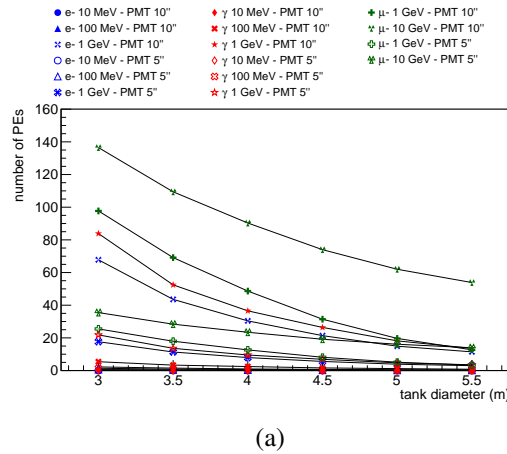
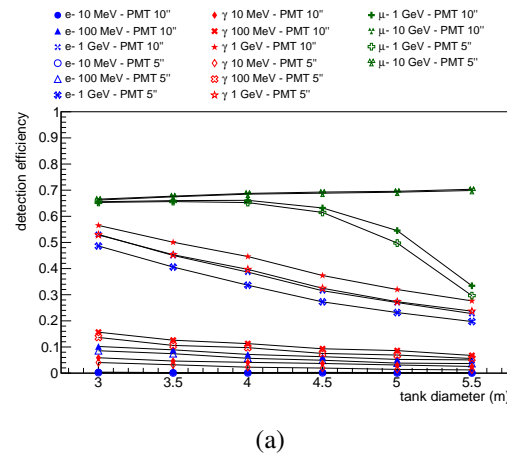**Figure 6.** Number of PEs detected in the lower layer of Circular-DLTs with reflective walls.

Figure 7. Detection efficiency of the lower layer of Circular-DLTs with reflective walls. In all the configurations, it is underestimated due to geometrical constraints.

the most commonly used shape for the construction of ground based astrophysical experiments due to their stronger strain resistance to the water pressure, ease of construction, and lower cost, tanks with square and the hexagonal bases have been considered because they would offer a higher fill factor, particularly important when it is necessary to cover areas with high density of tanks, like the inner array of the SWGO experiment.

The plots shown in this section represent the aforementioned parameters in function of the size of the tanks with different geometries and were made for 1 GeV particles, in order to compare the tank performance in the same conditions. The size of the tanks is represented by their width, i.e. diameter for Circular-DLTs, two times the side for Hexagonal-DLTs, and side for Square-DLTs. In figure 8–13 the performance of the upper layers of tanks with different shapes are shown, considering a central 10″ PMT or four peripheral 5″ PMTs. Panels (a) are relative to non-reflecting walls, while panels (b) are for reflecting walls. Similarly, in figure 14–17 the performance of the lower layer is

shown considering a 10″ PMT or a 5″ PMT. In the following, details about the comparison of the performance of the upper and lower layers are listed.

Performance of the upper layers.

- In general, Circular-DLTs and Hexagonal-DLTs produce a similar number of PEs, which is higher than for Square-DLTs by a factor ~ 1.5.

- With reflective walls, the number of PEs is about 3 times larger than that obtained with non-reflective walls, in any kind of tank (compare panels (a) with panels (b) in figure 8 and figure 9).

- Comparing the response of the central 10″ PMT and the four peripheral 5″ PMTs in the upper layer, the number of PEs for the first configuration is ~ 1.5 times higher than the number of PEs for the latter configuration for all tank geometries (compare panel (a) and panel (b) in figure 8 with the same panels in figure 9).

- The detection efficiency of the upper layer is similar for all kinds of tank. As already shown, it is higher using reflective walls (compare panels (a) with panels (b) in figure 10 and figure 11).

- Although the number of PEs is higher for the central 10″ PMT, the detection efficiency for 1 GeV particles is similar for both configurations of PMTs (compare panels (a) and (b) in figure 10 with those in figure 11).

- The time resolution of the measurement of the first photon considering the central 10″ PMT is ~ 0.5 ns larger than that of the four peripheral 5″ PMTs (compare panels (a) and panels (b) in figure 12 with those in figure 13). However, such values are slightly higher for Square-DLTs than the others.

- In general, with reflective walls the temporal resolution of the measurement of the first photon in upper layers is about 1 ns larger than with non-reflective walls, in all kinds of tanks (compare panels (a) with panels (b) in figure 12 and figure 13).

Performance of the lower layers.

- In the lower layer of the three kinds of tanks, the number of PEs is higher for Circular-DLTs and Hexagonal-DLTs than for Square-DLTs.

- The height of the lower layer influences the number of PEs, which is lower for 0.5 m but comparable for 0.75 m and 1 m (plots not shown in this work).

- The number of PEs produced by the 10″ PMT is 4 times that produced by the 5″ PMT, simply because of the ratio between the active areas of the sensors (see figure 14 and figure 15).

- Despite the difference in the number of PEs detected with the two PMT configurations, the detection efficiency of the lower layer does not vary (see figure 16 and figure 17).

- For Circular-DLTs and Hexagonal-DLTs the detection efficiency is similar and between ~ 10% and ~ 20% higher than for Square-DLTs, depending on the tank width. This is valid for the three simulated heights.
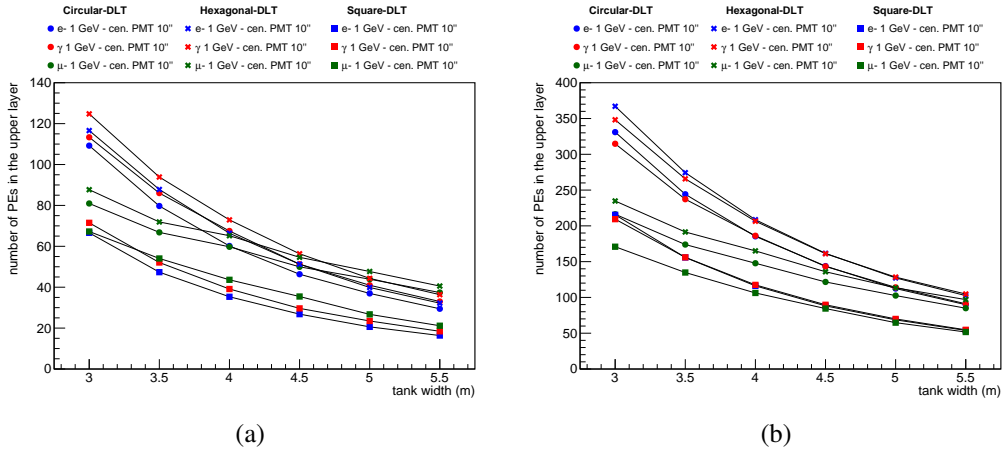
Figure 8. Comparison of the number of PEs detected in the upper layer with non-reflective walls (a) and reflective walls (b), for 1 GeV particles, for different geometries and considering only the central 10″ PMTs.
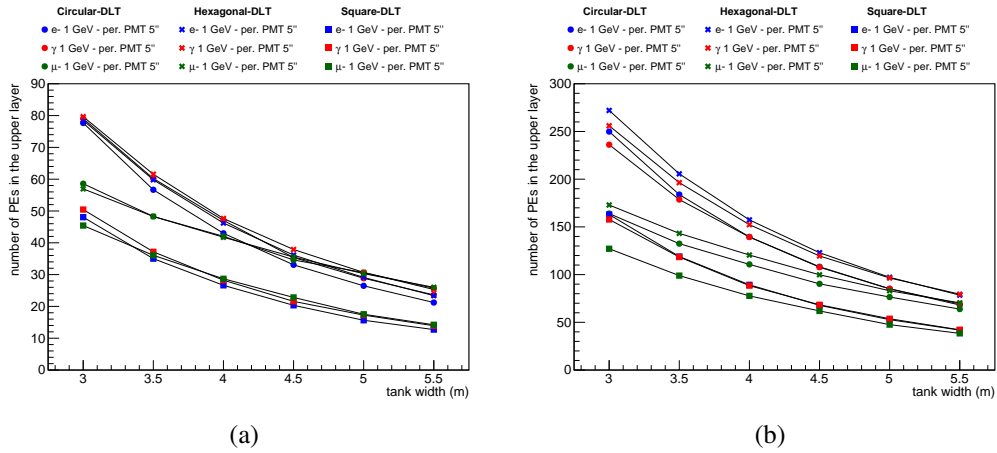

Figure 9. Comparison of the number of PEs detected in the upper layer with non-reflective walls (a), and reflective walls (b) for 1 GeV particles, for different geometries and considering only the peripheral 5″ PMTs.

- In all the configurations, the detection efficiency of the lower layer is underestimated in the same way due to geometrical constraints (see details about the calculation of the detection efficiency in section 3).

5 Conclusion

This study allowed to compare the response of double-layer tanks with different shape, i.e. with circular, hexagonal and square base of different size, to the passage of single particles of different type and energy. Moreover, it offered the possibility to compare tanks with reflective and non-reflective walls in the upper layer.

Regarding the performance of the upper layers, we found that:

- Regardless of the tank design and the reflective properties of the walls, the performance of the
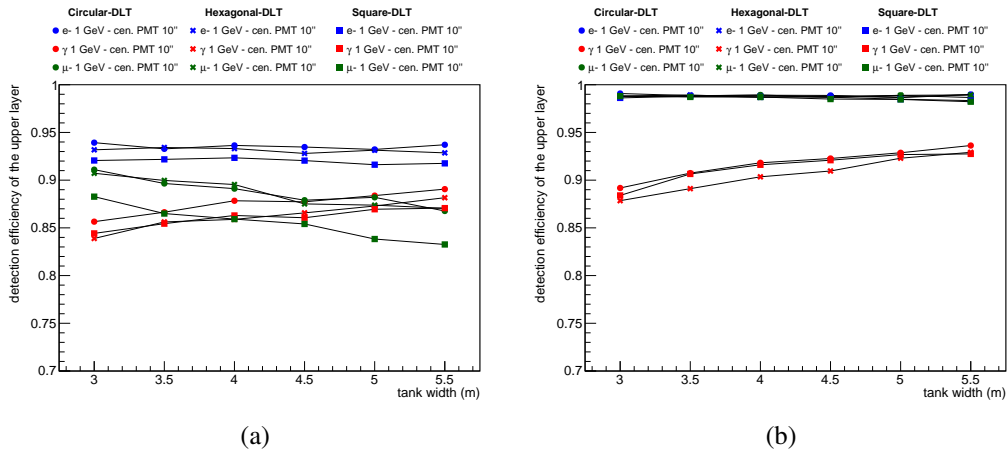
Figure 10. Comparison of detection efficiency of the upper layer with non-reflective walls (a) and reflective walls (b), for 1 GeV particles, for different geometries and considering only the central 10″ PMTs.
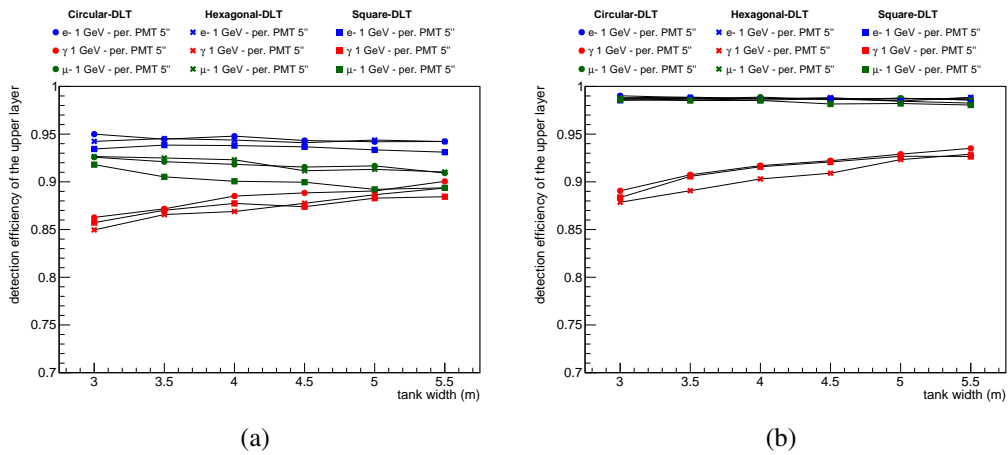

Figure 11. Comparison of the detection efficiency of the upper layer with non-reflective walls (a) and reflective walls (b), for 1 GeV particles, for different geometries and considering only the peripheral 5″ PMTs.

tanks worsen while increasing the width of the tank, because the "sensitive area", i.e. the area covered by the PMTs, decreases with respect to that of the base of the tank.

- With non-reflecting walls and 1 PE threshold, the detection efficiency for 10 MeV particles is between 30% and 15% depending on the tank width, while it is above 70% for higher energies and for all tank sizes, reaching values higher than 90% for 1 GeV and 10 GeV particles.

- With reflective walls, the number of PEs increases by a factor ~ 3. The detection efficiency for 10 MeV particles reaches values between $\sim 80\%$ and $\sim 50\%$ depending on the tank width, while it is above $\sim 90\%$ for all the higher energy particles. With 2 PEs threshold it is reduced by a few ten percent for 10 MeV and 100 MeV particles, while it is similar for particles with higher energy, for both non-reflective and reflective walls.
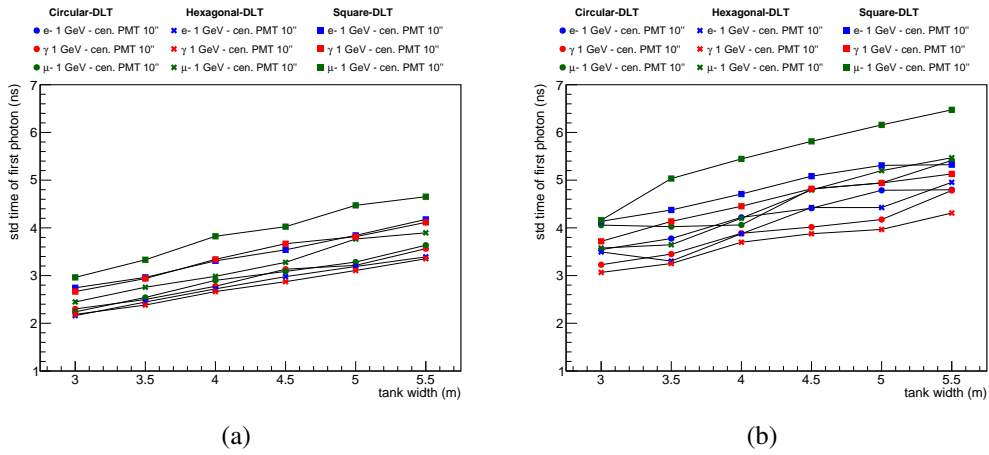
Figure 12. Comparison of the time resolution of the measurement of the first photon in case of non-reflecting walls (a) and reflective walls (b) in the upper layer, for 1 GeV particles, for different geometries and considering only the peripheral 10″ PMTs in the upper layer.
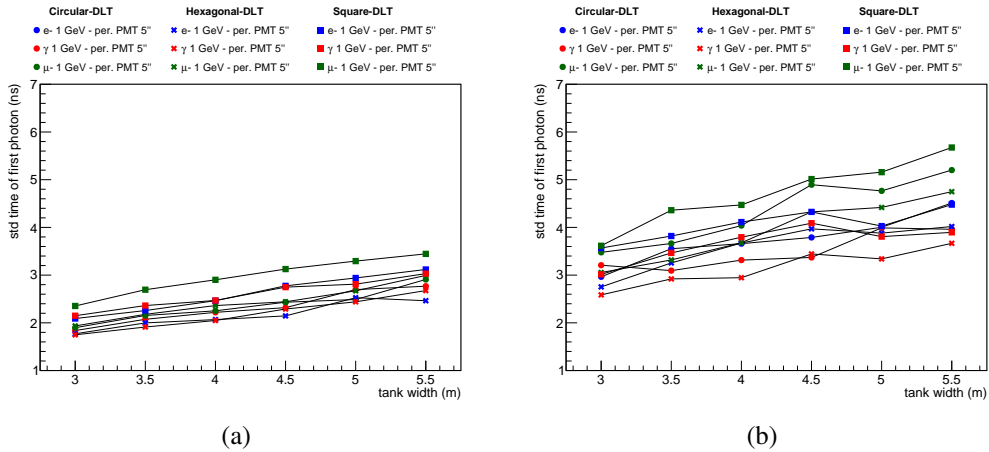

Figure 13. Comparison of the time resolution of the measurement of the first photon in case of non-reflecting walls (a) and reflective walls (b) in the upper layer, for 1 GeV particles, for different geometries and considering only the peripheral 5″ PMTs in the upper layer.

Considering the resolution of the measurement of the first photon:

- With 1 PE threshold ranges from ∼ 2.5 ns to ∼ 3.5 ns increasing the tank width.

- Using reflective walls, it slightly increases for 100 MeV and 1 GeV particles, and rises up to ∼ 18 ns for 10 MeV particles. It has similar values for the central 10″ PMT and the four peripheral 5″ PMTs. Considering 2 PEs threshold, it has slightly lower values.
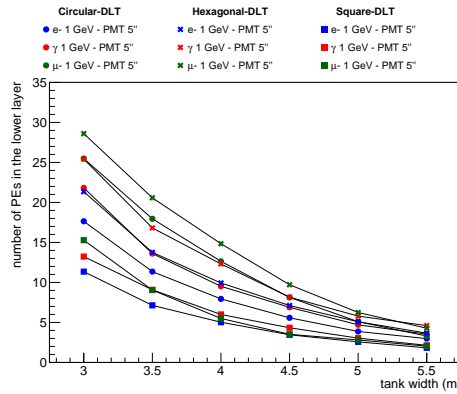
Regarding the performance of the lower layers:

- Like in the upper layer, the number of detected PEs and the detection efficiency in the lower layers decrease with the size of the tank.
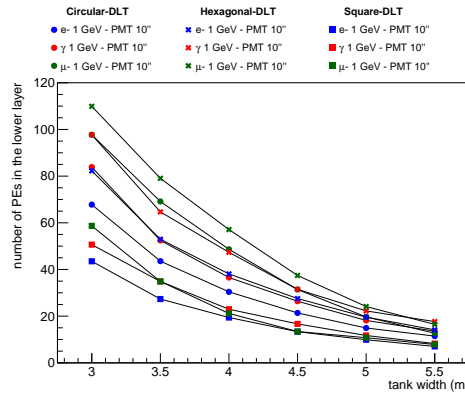
Figure 14. Comparison of the number of PEs in the lower layer with reflective walls, for 1 GeV particles, for different geometries and considering the 10″ PMT.

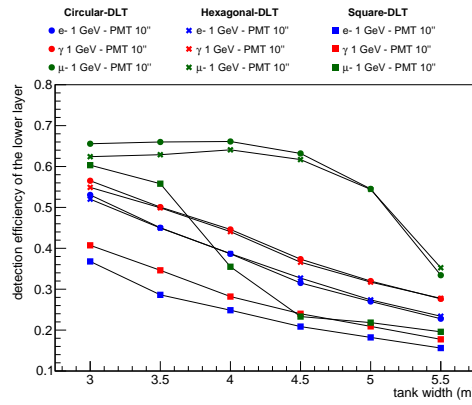**Figure 15.** Comparison of the number of PEs in the lower layer with reflective walls, for 1 GeV particles, for different geometries and considering the 5″ PMT.

- Electrons and gamma-rays of 10 MeV and 100 MeV are rarely detected in lower layers, with an efficiency lower than 15%, while with energy of 1 GeV varies between ∼ 50% and ∼ 30% increasing the tank width. For muons it is ∼ 65% for both 1 GeV and 10 GeV up to tanks with 4 m width then, for increasing tank dimensions, it decreases for the 1 GeV muons while remains constant for the 10 GeV ones. These values are underestimated in the same way due to geometrical constraints.

- The height of the lower layer influences the number of PEs, which is comparable for 0.75 m and 1 m and lower for 0.5 m, but does not affect the detection efficiency.

Comparing the performance of different PMT configurations:

- In the upper layer, the central 10″ PMT produces more PEs than the four peripheral 5″ PMTs, although both sensitive areas are similar, but the detection efficiencies are comparable. This is related to the position of the PMTs.

(a)

Figure 16. Comparison of the detection efficiency of the lower layer with reflective walls, for 1 GeV particles, for different geometries and considering the 10″ PMT. In all the configurations, it is underestimated due to geometrical constraints.
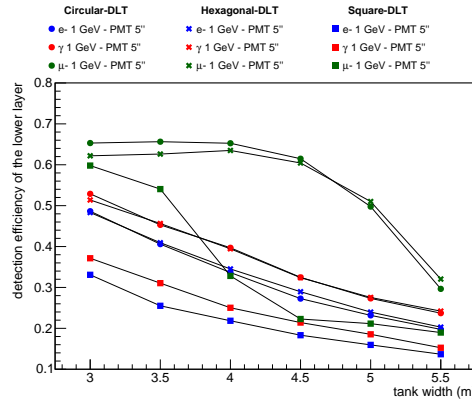
(a)

Figure 17. Comparison of the detection efficiency of the lower layer with reflective walls, for 1 GeV particles, for different geometries and considering the 5″ PMT. In all the configurations, it is underestimated due to geometrical constraints.

- In the lower layer, the 5″ PMT produces a number of PEs that is 25% of that produced in the 10″ PMT, being proportional to the area of the photocathode, but the detection efficiencies are similar.

The comparison of the performance of tanks with different geometries revealed that:

- In general, in the upper layer Circular-DLTs and Hexagonal-DLTs produce a similar number of PEs, which is ∼ 1.5 times higher than for Square-DLTs. However, the detection efficiency of the upper layer is similar for all kinds of tank.

- The width of the first photon time distribution is slightly wider for Square-DLTs than the others.

- For Circular-DLTs and Hexagonal-DLTs the detection efficiency of the lower layer is similar and between ∼ 10% and ∼ 20% higher than for Square-DLTs, depending on the tank width. It is similar for the three different heights considered for the lower layer.

Beside to the performance of tanks with different geometries, for the final design of ground based astrophysical observatories like the SWGO array it should be taken into account also that with Hexagonal-DLTs and Square-DLTs it is possible to achieve a higher fill factor, although they are potentially more expensive solutions.

References

[1] U. Barres de Almeida, *The Southern Wide-Field Gamma-ray Observatory*, *Astron. Nachr.* **342** (2021) 431 [arXiv:2012.13740].

[2] J. Hinton, *The Southern Wide-field Gamma-ray Observatory: Status and Prospects*, *PoS* **ICRC2021** (2021) 023 [arXiv:2111.13158].

[3] HAWC collaboration, *The HAWC observatory*, *Nucl. Instrum. Meth. A* **692** (2012) 72.

[4] LHAASO collaboration, *The Large High Altitude Air Shower Observatory (LHAASO) Science Book (2021 Edition)*, *Chin. Phys. C* **46** (2022) 035001 [arXiv:1905.02773].

[5] S. Kunwar, *Double-layered Water Cherenkov Detector for SWGO*, *PoS* **ICRC2021** (2021) 902.

[6] H. Schoorlemmer, R. Conceição and A.J. Smith, *Simulating the performance of the Southern Wide-view Gamma-ray Observatory*, *PoS* **ICRC2021** (2021) 903.

[7] J. Allison et al., *Geant4 developments and applications*, *IEEE Trans. Nucl. Sci.* **53** (2006) 270.

[8] Datasheet of the Hamamatsu PMT models, https://www.hamamatsu.com/content/dam/hamamatsu-photonics/sites/documents/99_SALES_LIBRARY/etd/LARGE_AREA_PMT_TPMH1376E.pdf

[9] HAWC collaboration, *Highlights from HAWC*, *EPJ Web Conf.* **208** (2019) 14001.

[10] P.A. Amaudruz, M. Batygov, B. Beltran, C.E. Bina, D. Bishop, J. Bonatt et al., *In-situ characterization of the Hamamatsu R5912-HQE photomultiplier tubes used in the DEAP-3600 experiment*, *Nucl. Instrum. Meth. A* **922** (2019) 373 [arXiv:1705.10183].